First Principles Quantum Mechanics Methods for Simulating Fundamental Phenomena in Batteries and Fuel Cells

Emily A. Carter
carter.princeton.edu
acee.princeton.edu

Batteries

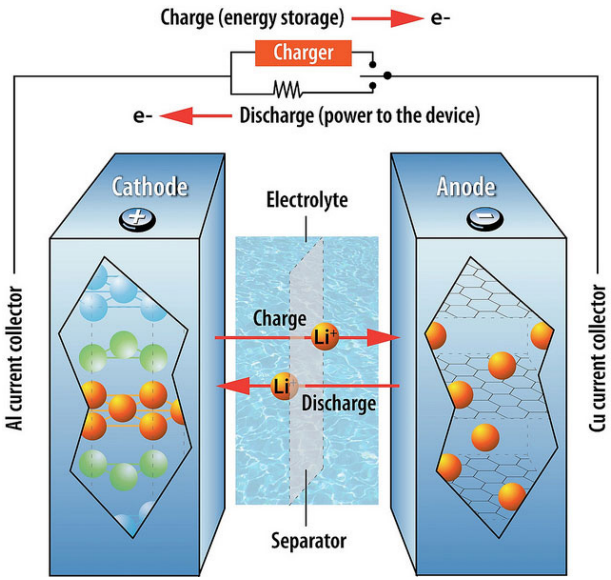

Fuel Cells

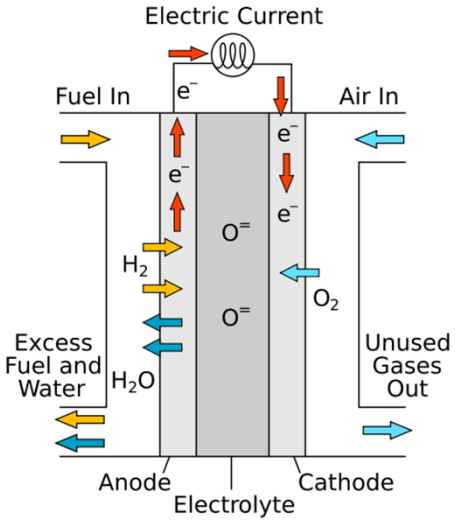

- Complex charge transfer and mechanical deformation processes
- In situ spectroscopic expts nearly nonexistent – theory needed...
- Here: Embedded Correlated Wavefunction theory and Orbital-Free DFT

Embedded Correlated Wavefunction (ECW) Theory

For molecule-surface interactions:

- Use periodic DFT for extended surface

- Locally use correlated wavefunction (CW) methods subject to embedding potential to correct the DFT energies

Embedded energy for total system:

$$E_{\text{tot}}^{\text{emb}} = E_{\text{total}}^{\text{DFT}} + \underbrace{\left(E_{\text{cluster}}^{\text{CW}} - E_{\text{cluster}}^{\text{DFT}}\right)}_{\text{Embedded}}$$

Current embedding schemes

Partition system into subsystems interacting via global embedding potential:

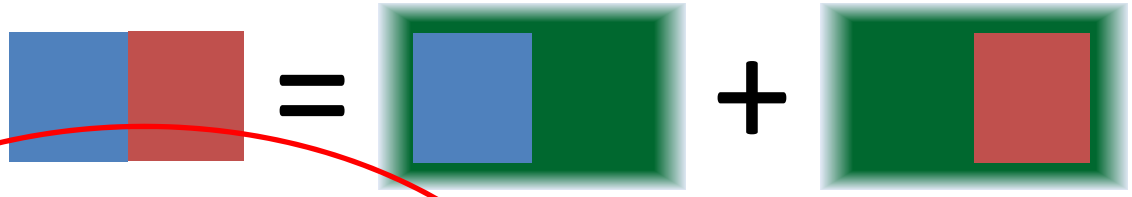

Density-based embedding:

Unique exact embedding potential defined such that summed subsystem densities reproduce total density

$$\sum \rho_i[V_{\text{emb}}] = \rho_{\text{ref}}$$

Keep potential fixed for subsequent high level calculations in subsystems

C. Huang, M. Pavone, and E. A. Carter, *J. Chem. Phys.*, **134**, 154110 (2011)

Potential-functional embedding:

Find embedding potential that minimizes total energy

$$\min_{V_{\text{emb}}} E\left[\rho_i\left[V_{\text{emb}}\right]\right]$$

Self-consistent minimization of energy, allow for self-consistent back-action

C. Huang and E. A. Carter, *J. Chem. Phys.*, **135**, 194104 (2011)

Density-based embedding theory

Partition system into cluster of interest and surrounding environment

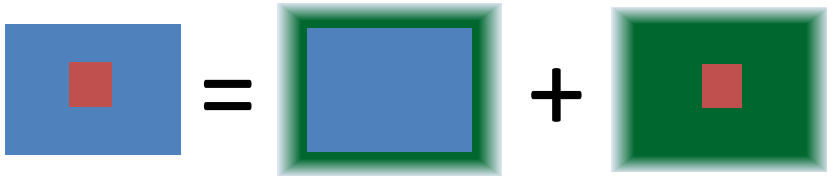

V_{emb}

$$E_{\text{tot}}[\rho_{\text{total}}] = E_{\text{cluster}}[\rho_{\text{cluster}}] + E_{\text{env}}[\rho_{\text{env}}] + E_{\text{int}}[\rho_{\text{total}}, \rho_{\text{cluster}}, \rho_{\text{env}}]$$

$$W_{\text{emb}}^{\text{cluster}\to\text{env}}(\vec{r}) = \frac{\delta E_{\text{int}}}{\delta \rho_{\text{cluster}}} = \frac{\delta E \delta E_{\text{int}}}{\delta \rho_{\text{env}} \delta \rho_{\text{env}}} \qquad V_{\text{emb}}^{\text{env}\to\text{cluster}}(\vec{r}) = \frac{\delta E_{\text{int}}}{\delta \rho_{\text{cluster}}}$$

Define unique embedding potential

Optimization with Lagrange multipliers: reproduce target density ρ_{ref}

$$W[\rho_{\text{cluster}}, \rho_{\text{env}}, V_{\text{emb}}] = E_{\text{cluster}}[\rho_{\text{cluster}}] + E_{\text{env}}[\rho_{\text{env}}] + \int V_{\text{emb}}(\vec{r})\left(\rho_{\text{cluster}} + \rho_{\text{env}} - \rho_{\text{ref}}\right) dr^3$$

$\rho_{cluster}$ is the solution of: $E_{\text{cluster,emb}}[\rho_{\text{cluster}}, V_{\text{emb}}] = E_{\text{cluster}}[\rho_{\text{cluster}}] + \int V_{\text{emb}}(\vec{r})\rho_{\text{cluster}}(\vec{r}) dr^3$

ρ_{env} is the solution of: $E_{\text{env,emb}}[\rho_{\text{env}}, V_{\text{emb}}] = E_{\text{env}}[\rho_{\text{env}}] + \int V_{\text{emb}}(\vec{r})\rho_{\text{env}}(\vec{r}) dr^3$

Q. Wu and W. Yang Phys. Rev. Lett. **89**, 143002 (2002)

C. Huang, M. Pavone, and E. A. Carter, J. Chem. Phys., **134**, 154110 (2011)

ECW Theory Applications

- Fuel Cell Catalysis
  - Model Oxygen Reduction Reaction: O_2 on Al (111)
- Photoelectrochemical Catalysis
  - Plasmon-induced H_2 dissociation on Au nanoparticles

O_2/Al(111): Experiments

Measure O_2 sticking on clean Al (111) surface

Surprising result:
saturation only sets in at incident energies above 600 meV

Activation barrier involved

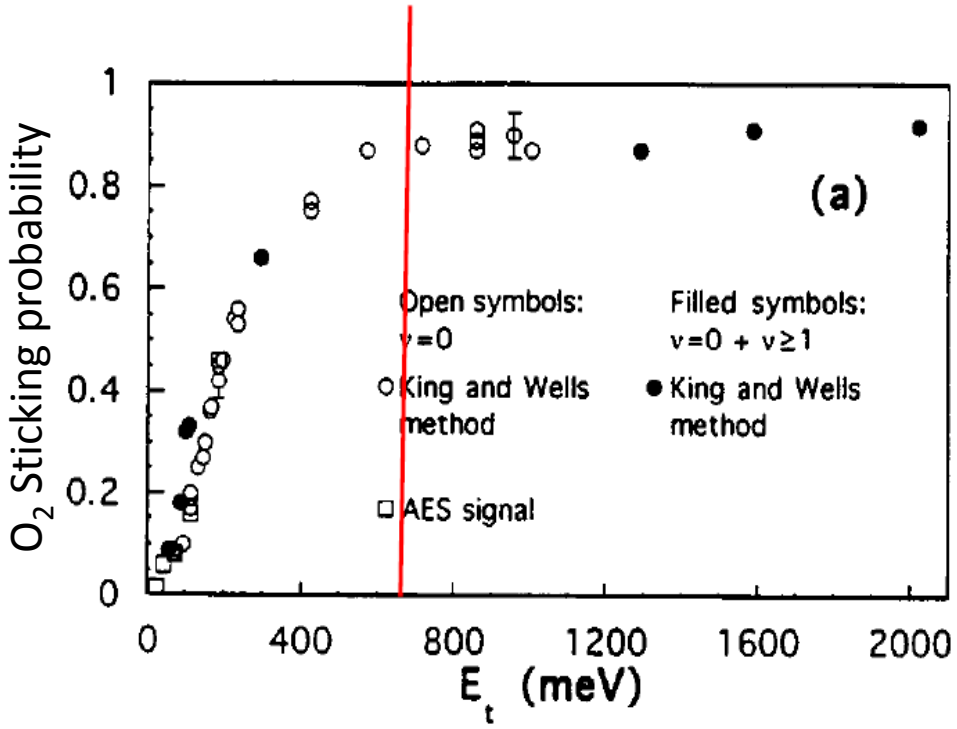

L. Österlund et al., PRB **55**, 15452 (1997)

O_2/Al(111): Experiments

STM analysis:

- Both single oxygen atoms and pairs on the surface.
- Singles / Pairs ratio depends on incident energy.

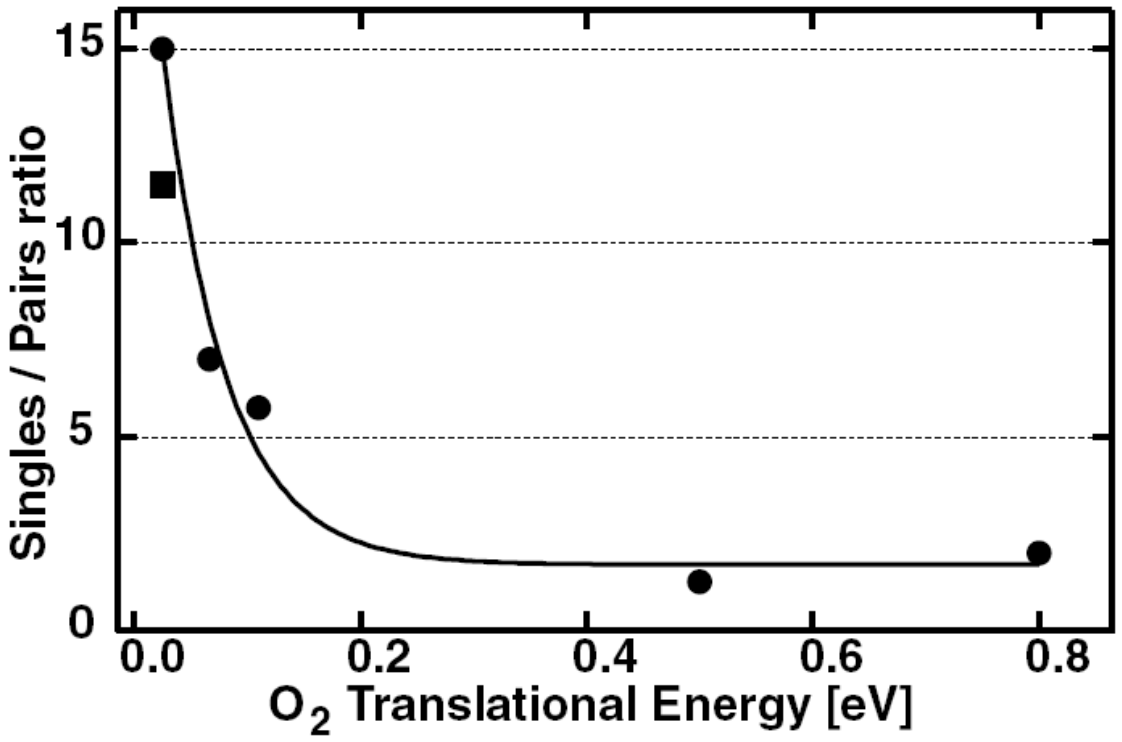

Possible explanations:

- Hot O-atoms move on Al surface
- Abstraction process: dissociative sticking

H. Brune et al., PRL **68**, 624 (1992)
Komrowski et al., PRL **87**, 246103 (2001)

O_2/Al(111): Theory

Initial DFT studies predict no activation barrier

Honkala et al. Phys.Rev.Lett. **84**, 705 (2000), Yourdshahyan et al., Phys.Rev.B **65**, 75416 (2002)

Diabatic surface hopping based on quasi-empirical potential energy surfaces

Barrier due to dynamics of charge transfer

Katz et al. J.Chem.Phys. **120**, 3931 (2004)

Spin constraints and revised PBE functional: barriers still too small

Behler et al. Phys.Rev.Lett. **94**, 036104 (2005), Behler et al. Phys.Rev.B **77**, 115421 (2008)

O_2 + cluster of 4-5 Al atoms

CASSCF or hybrid XC functionals: finite barrier (~350 meV) but still too small

DFT fails because of self-interaction error

Livshits et al. J. Phys. Chem. A **113**, 7526 (2009), C. Mosch et al., J. Phys. Chem. C **112**, 6924 (2008)

Here: use embedding theory that treats extended metal surface with DFT and adsorbate-metal interaction with correlated wavefunction theory

Huang et al. *J. Chem. Phys.* **134**, 154110 (2011)

Bridge PES: dissociative chemisorption

Contour separation 200 meV

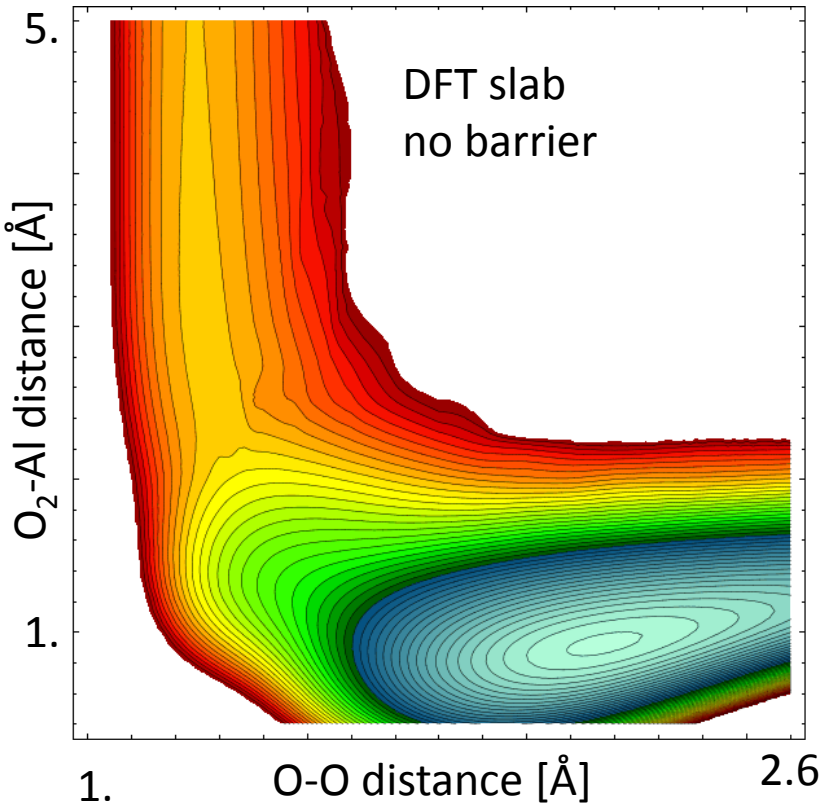

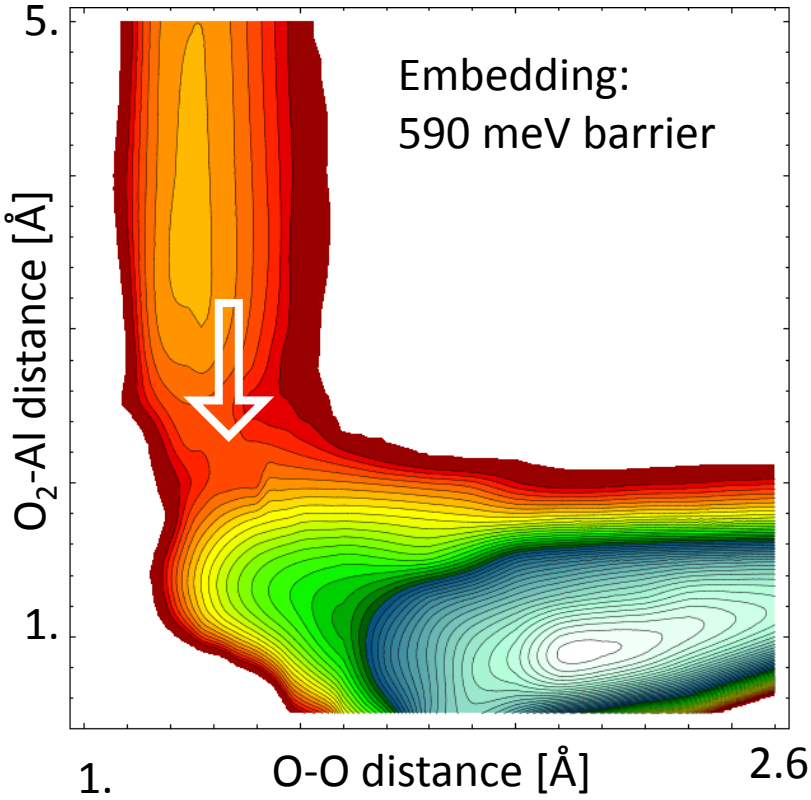

F. Libisch, C. Huang, P. Liao, M. Pavone, and E. A. Carter, Phys. Rev. Lett. **109**, 198303 (2012)

Charge transfer

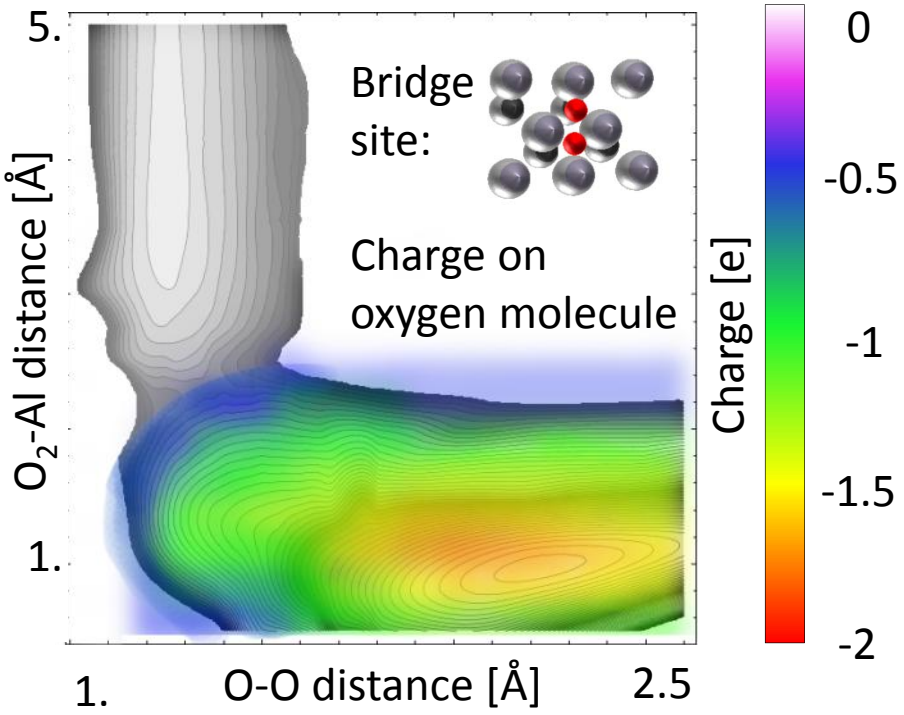

- Abrupt charge transfer at barrier crossing
- Origin of barrier: energy to initiate charge transfer (O_2 loses resonance, Al work fcn)
- DFT calculation features smooth charge transfer -> no barrier

- As charge transfers, O_2 local spin state appears to change from triplet to singlet (bonds forming to surface, and more…)

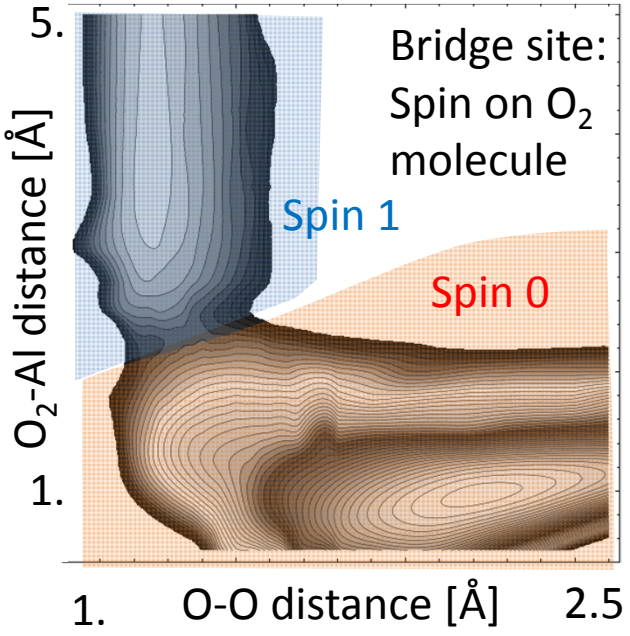

FCC PES: oxygen abstraction

Contour separation 200 meV

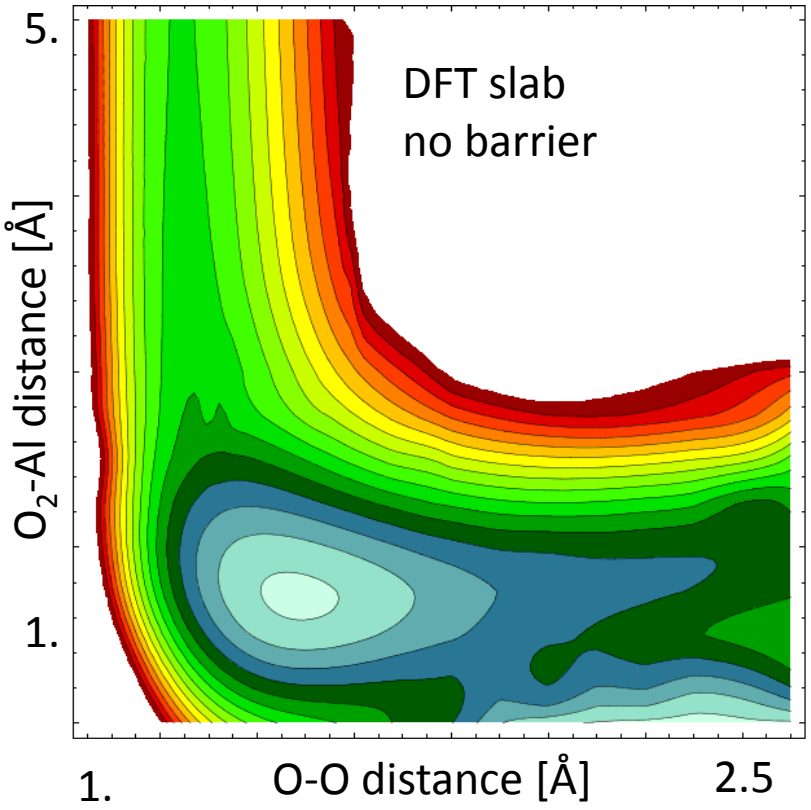

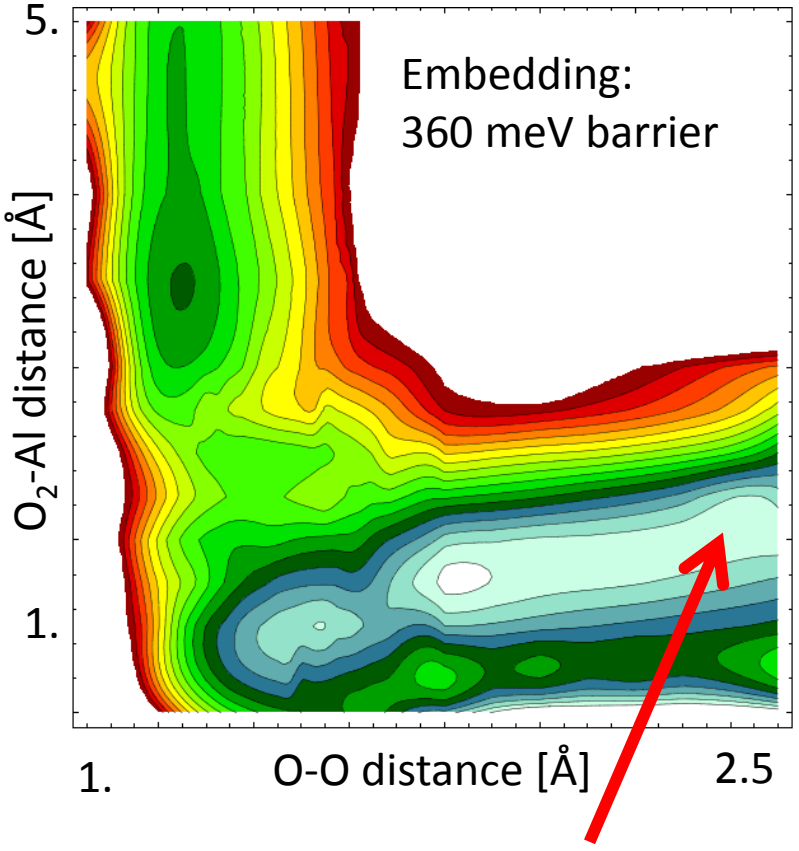

Abstraction
Not accounted for by DFT

What is origin of barrier?

- What happens at top of the barrier?
- Oxygen charge and spin jump discontinuously in ECW theory
- Abrupt O spin and charge change not reproduced by DFT

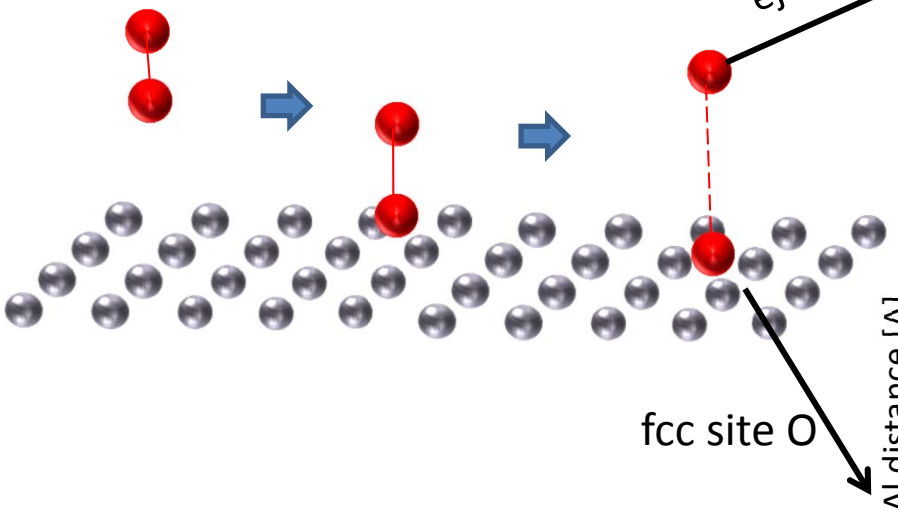

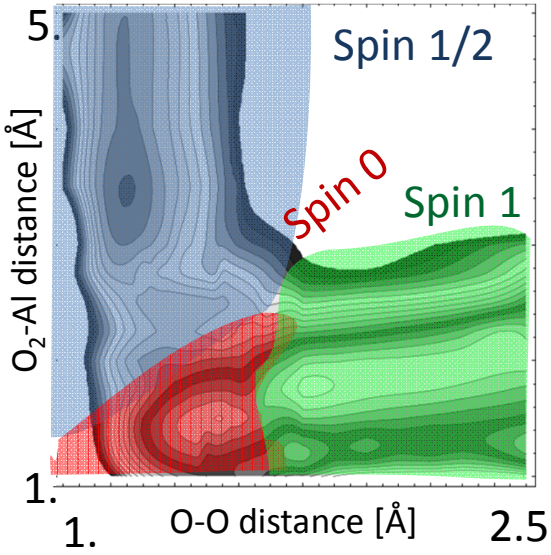

Charge on ejected O is 0.0±0.2 e

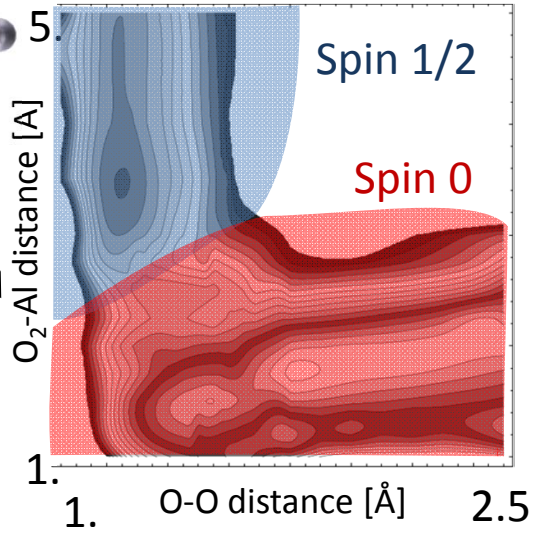

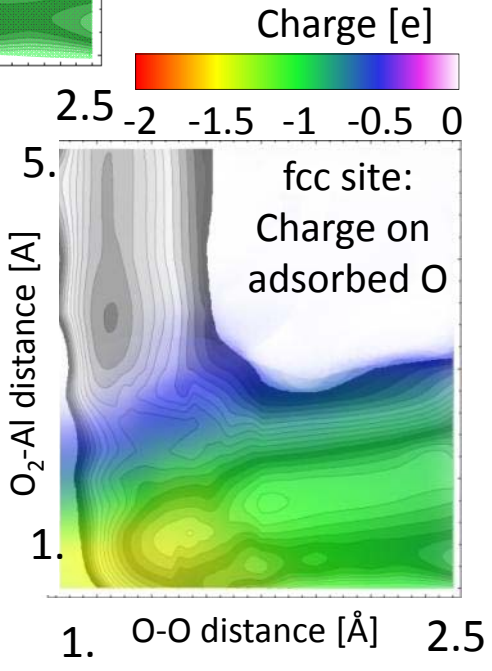

Spin quantum number

- Scheffler et al. suggest different spin states as barrier origin: our results do not confirm this
- Difference between singlet and triplet surface?
- We calculate both PESs and find almost no difference
- CASPT2 calculation of isolated O_2 for lowest singlet ($^1\Delta_g$) and triplet ($^3\Sigma_g^-$) states shows (correct) energy splitting of 1.4 eV
- However, lowest spin excitation of embedded metal cluster (embedded CASPT2, without O_2) is 0.12 eV
- Explanation: O_2 always in triplet state. Embedded metal cluster provides additional spin to get required S^2 of entire system
- Since an infinite metal surface requires even lower energy to flip a spin, our barrier might be too high by 0.12 eV

Activation barriers

F.Libisch, C. Huang, P. Liao, M. Pavone, and E. A. Carter, Phys. Rev. Lett. **109**, 198303 (2012)

Site	Atoms (1^{st}/2^{nd} layer)	Orientation	Barrier [meV]
Bridge	4/4	parallel	1060
Bridge	8/4	parallel	540
Bridge	8/6	parallel	590
Bridge		perpendicular	450
FCC	6/6	parallel	430
		perpendicular	360
HCP	6/6	parallel	410
		perpendicular	410
TOP	7/3	parallel	660
		perpendicular	660

- Small clusters overestimate barrier: need more than 10 atoms
- Largest converged barriers: 660 meV
- Lowest barrier for perpendicular incidence: abstraction at low energies!

Comparison to experiment

- King-Wells sticking saturates at ~600 meV
- Our largest PES barriers at ~650 meV

- STM finds single adsorbed O-atoms
- PES for perpendicular incidence confirms abstraction mechanism

- At lower energies, single O atoms dominate
- PES features lowest barrier for perpendicular incidence: earlier charge transfer to closer O atom

- Recent hexapole-oriented O_2 King-Wells: parallel O_2 dominates sticking below 350 meV (n.b. – no measurement of product – molecular chemisorption?)

Kurahashi and Yamauchi, PRL, **110**, 246102 (2013)

L. Österlund et al., PRB **55**, 15452 (1997)

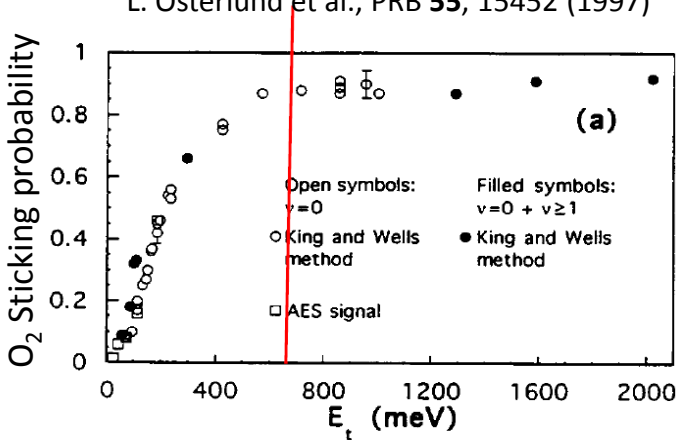

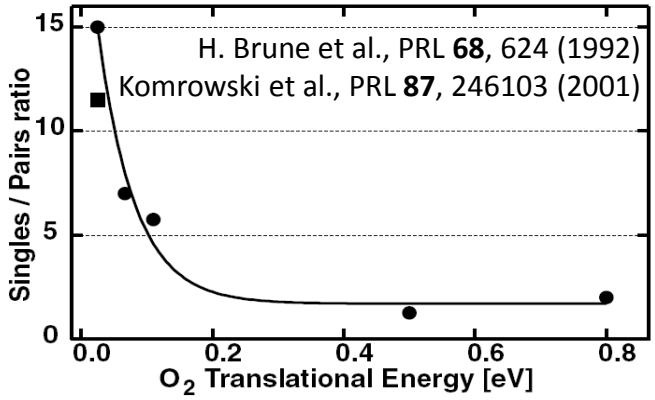

Conclusions

- ECW theory properly treats O_2 , charge transfer (CT), and excited states, unlike DFT
- O_2 on Al (111):
  - Barrier due to abrupt CT. Barrier height: cost of CT
  - CT in DFT too easy (self-interaction error/lack of derivative discontinuity in XC functional)
  - Low energy spin excitations of metal surface enable spin changes, captured by ECW theory , no need for artificial spin constraints
  - Experimental observables reproduced: ~600 meV barrier and abstraction at low energies (early CT origin of reduced barrier)

Density Functional Theory

$$E_{DFT}[\rho(\vec{r})] = T_S[\rho(\vec{r})] + J_{ee}[\rho(\vec{r})] + E_{XC}[\rho(\vec{r})] + \int V_{ext}(\vec{r})\rho(\vec{r})dr^3$$

How to accurately simulate matter without wavefunctions?
Challenges: electron kinetic energy and electron-ion interaction

In Kohn-Sham DFT

$$T_S[\rho(\vec{r})] = -\frac{1}{2}\sum_{i=occ}\int \psi_i^*(\vec{r})\nabla^2\psi_i(\vec{r})dr^3$$

$$\rho(\vec{r}) = \sum_i f_i\psi_i^*(\vec{r})\psi_i(\vec{r})$$

(1) Introduce orbitals. Must orthogonalize.

(2) Computational cost is usually ~ $O(N_{basis}*N_{orb}^2)$.

(3) Linear-scaling KS-DFT: localized basis sets or locally truncated KS equations → large prefactor & not applicable to metals.

In Orbital-Free DFT

$$T_{TF} = \frac{3}{10}\left(3\pi^2\right)^{2/3}\int \rho^{5/3}(\vec{r})dr^3$$

Thomas-Fermi kinetic energy density functional (KEDF)

$$T_{vW} = \frac{1}{8}\int \frac{|\nabla\rho(\vec{r})|^2}{\rho(\vec{r})}dr^3$$

von Weizsäcker KEDF

(1) Basic variable is the electron density.

(2) Computational cost can be made to ~$O(N \ln N)$.

(3) Local and semilocal KEDFs not accurate => Improve accuracy by adding nonlocal term.

How to accurately simulate matter without wavefunctions?

$$E_{OF-DFT}[\rho(\vec{r})] = T_S[\rho(\vec{r})] + J_{ee}[\rho(\vec{r})] + E_{XC}[\rho(\vec{r})] + \int V_{ext}(\vec{r})\rho(\vec{r})dr^3$$

Specific challenges:

Nonlocality of electron-ion interaction and electron kinetic energy

Quick history of Carter group contributions:

1999 – WGC99 nonlocal KEDF for *main group metals* (correct linear response; nearly as accurate as KS-DFT and orders of magnitude faster)

$$T_S = T_{TF} + T_{vW} + T_{nonlocal}$$

$$T_{nonlocal} = \iint \rho^{\alpha}(\vec{r})\Omega(\vec{r};\vec{r}')\rho^{\beta}(\vec{r}')dr^3dr'^3$$

$$\frac{1}{\tilde{\chi}(\mathbf{q})} = -\tilde{F}\left(\frac{\delta^2 T_s[\rho]}{\delta\rho(\mathbf{r})\delta\rho(\mathbf{r}')}\right)$$

2004 – Bulk-derived local pseudopotentials (BLPSs) for electron-ion interactions

2009 – Fully linear scaling/parallel code for science of many thousands of atoms

2010 – HC10 nonlocal KEDF for *covalent materials* (correct linear response; C. Huang and EAC, Phys. Rev. B **81**, 045206 (2010))

2012 – HC10 KEDF for *molecules* (J. Xia, et al., J. Chem. Phys. **136**, 084102 (2012))

2012 – Density-decomposed nonlocal KEDFs for *transition metals and semiconductors* (C. Huang and EAC, Phys. Rev. B **85**, 045126 (2012) and J. Xia and EAC, PRB **86**, 235109 (2012))

2013 - Transition metals via angular-momentum-dependent AMD-OFDFT (Y. Ke, F. Libisch, J. Xia, and EAC, *Phys. Rev. Lett.* **111**, 066402 (2013))

OFDFT Algorithmic Improvements: Linear Scaling and Parallelism

- Left: Pre-2009 OFDFT is O(NlnN) only for electron terms.
- Ion-ion and electron-ion terms $O(N^2)$ due to structure factor
- Right: OFDFT w/cardinal b-spline interpolation S(q) as in PME $\tilde{S}(\boldsymbol{q}) = \sum_{I=1}^{N_{\text{ion}}} e^{-2\pi i \boldsymbol{q}\cdot\boldsymbol{R}_I}$

L. Hung and EAC, Chem. Phys. Lett., **475**, 163 (2009)

Choly and Kaxiras, Phys. Rev. B 67, 155101 (2003).

Essman, Perera, and Berkowitz, J. Chem. Phys. **103**, 15 (1995).

Previous code

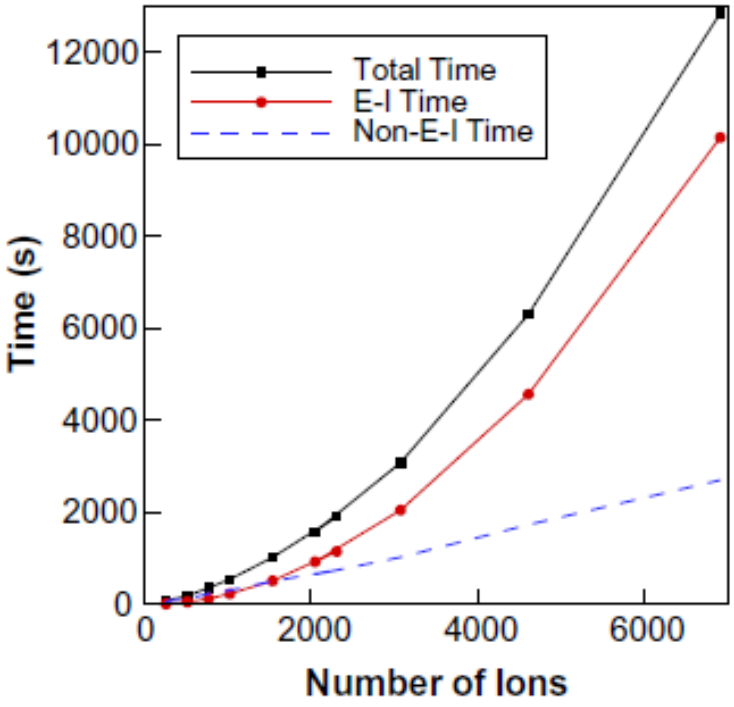

Current code

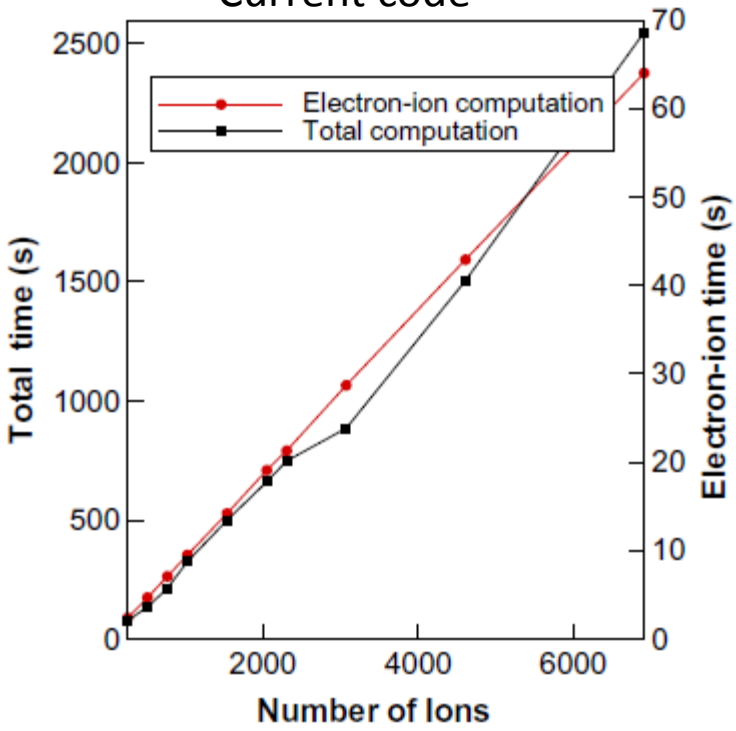

Code parallelized via domain decomposition of the electron density.

Benchmark OFDFT calculations on > 1M atoms: 5.5 hrs on <200 processors in 2009

Mechanical Deformation Controlled by Dislocation Properties

Elastic moduli

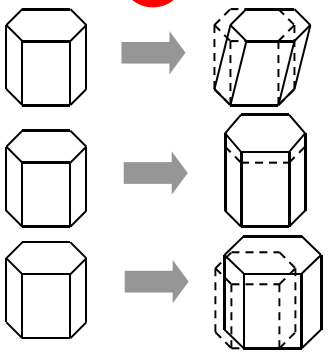

KSDFT

Generalized Stacking Fault Energy (SFE)

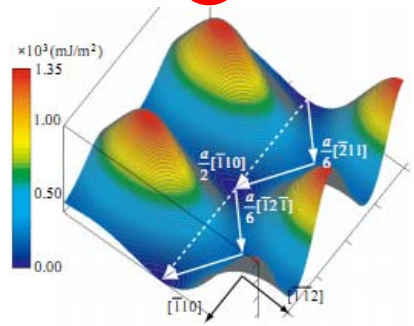

KSDFT

Dislocation structure

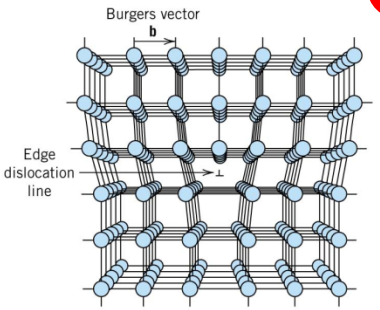

OFDFT

OFDFT

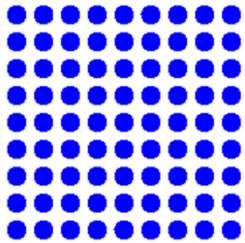

Dislocation mobility

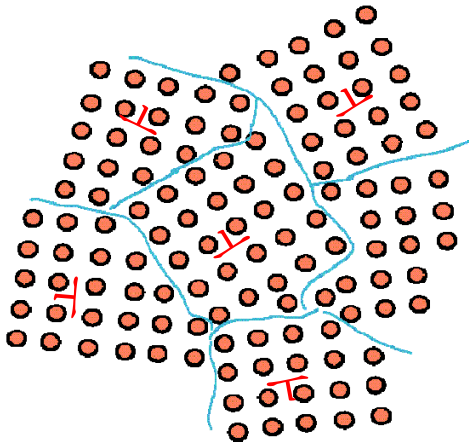

Stacking Fault Energy Surfaces for Mg Slip Systems: KSDFT vs OFDFT versus Classical EAM Potentials

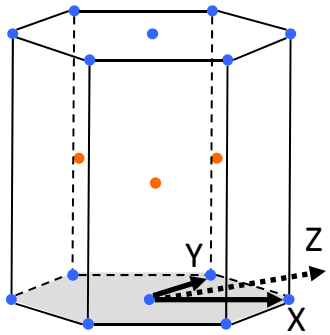

Basal {0001}<11-20>

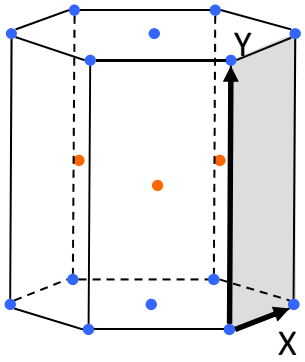

Prismatic {1-100}<11-20>

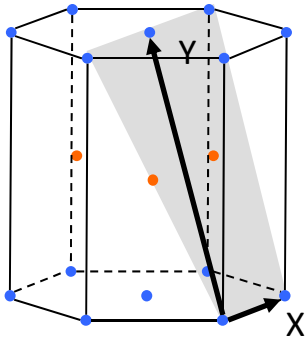

Pyramidal {1-101}<11-20>

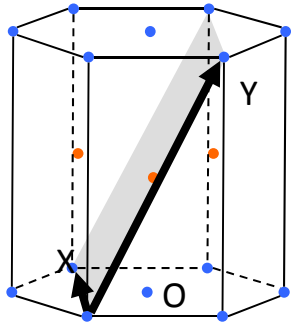

Pyramidal <c+a> {-2112}<2-1-13>

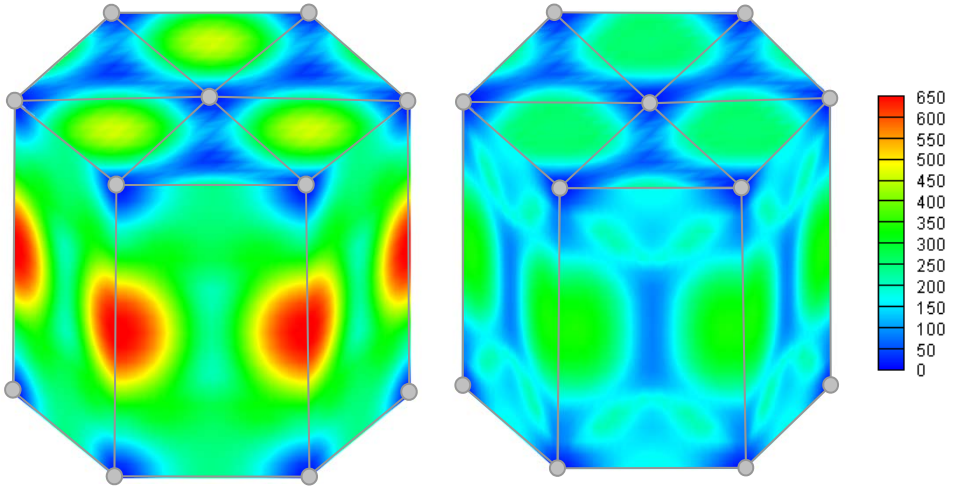

OFDFT **EAM**

EAM incorrectly predicts favorable cross-slip

Prismatic GSFE

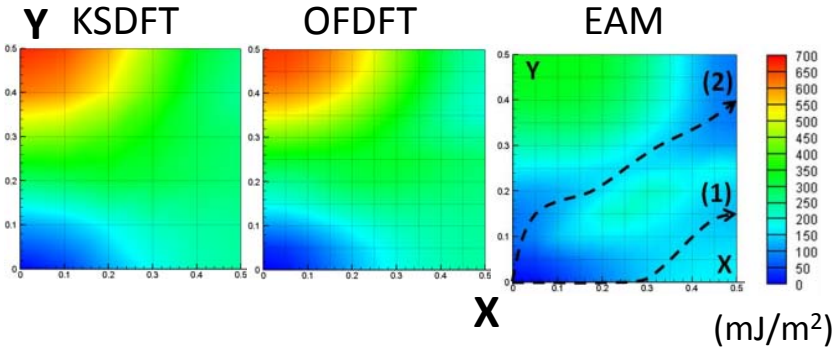

(mJ/m²)

- **Mg slip systems are very anisotropic.**
- **QM needed to accurately study plasticity of HCP Mg.**

I. Shin and EAC, *Modell. Simul. Mater. Sci. Eng.*, **20**, 015006 (2011).

Li-ion battery: components

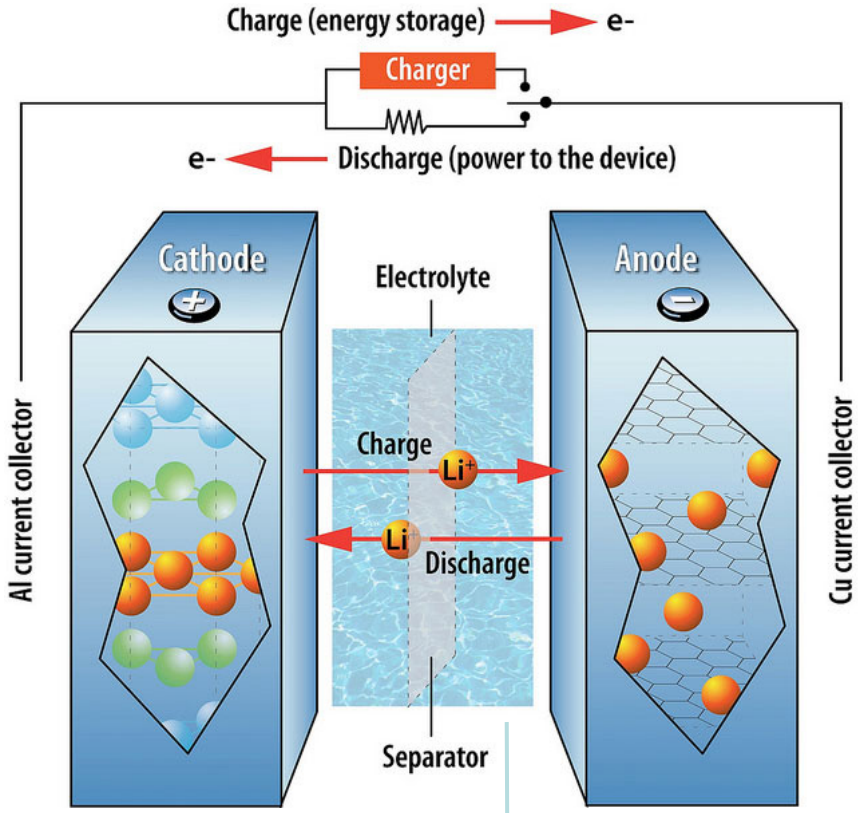

Cathode: metal oxide
$LiCoO_2$, $LiMnO_2$, $LiNiO_2$

Anode: graphite

Electrolyte: liquid or solid
Mixture of Li salt and esters, ethers and carbonates, etc.

$$\text{Cathode:}\quad LiMO_2 \underset{\text{Discharge}}{\overset{\text{Charge}}{\rightleftharpoons}} Li_{1-x}MO_2 + xLi^+ + xe$$

$$\text{Anode:}\quad C + xLi^+ + xe \underset{\text{Discharge}}{\overset{\text{Charge}}{\rightleftharpoons}} Li_xC$$

$$\text{Overall:}\quad LiMO_2 + C \underset{\text{Discharge}}{\overset{\text{Charge}}{\rightleftharpoons}} Li_xC + Li_{1-x}MO_2$$

Anode: silicon vs. graphite

Pros:

- greater lithium capacity:
  $Li_{22}Si_5$ ≈ 4200 mAh/g
  Graphite ≈ 372 mAh/g
- lower self heating rate
- safer

Cons:

- low intrinsic electrical conductivity
- poor cycling performance:
  400% volume change vs. 10% in graphite
  severe structure change

fracture, disconnection, capacity loss

Can WGC99 KEDF Model Bulk Si?

	CD	HD	cbcc	β tin	bct5	sc	hcp	sbcc	fcc
KS BLPS									
V_0 (Å^3)	19.432	19.492	17.850	14.880	16.838	15.537	13.858	14.058	14.022
B_0 (GPa)	95.5	91.5	90.0	106.5	97.5	103.0	83.0	88.6	87.8
$(\Delta)E_{\min}$ (eV/atom)	−110.234	0.020	0.165	0.275	0.249	0.303	0.447	0.462	0.457
OF BLPS, optimal γ,ρ_*									
V_0 (Å^3)	21.585	19.676	18.372	15.098	17.695	16.156	13.713	13.965	13.763
B_0 (GPa)	60.9	76.7	87.9	104.4	77.8	95.5	109.6	105.4	99.8
$(\Delta)E_{\min}$ (eV/atom)	−110.220	0.288	0.267	0.361	0.307	0.308	0.443	0.490	0.444

Table and plot from ref. 1

- Inaccurate energy differences for Si semiconductor phases.
- Even worse for III-V semiconductors.
- Divergence in minimization.

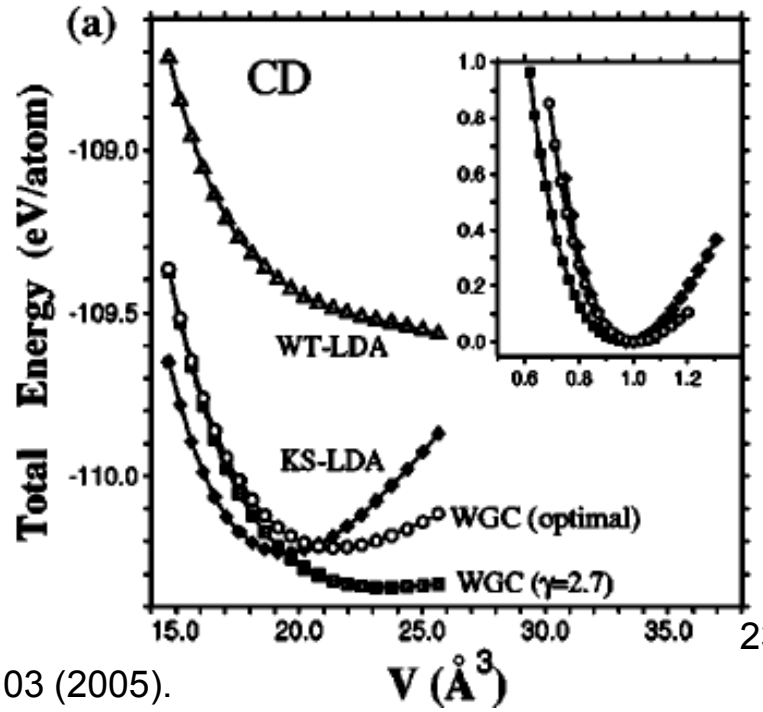

1. B. Zhou, V. Ligneres, and EAC, *J. Chem. Phys*. **122**, 044103 (2005).

DENSITY-DECOMPOSED WGC KEDF FOR SEMICONDUCTORS

- Density fluctuations in Si phases:

Si	CD	HD	cbcc	β-tin	bct5	sc	hcp	bcc	fcc	Al fcc
ρ_{max}/ρ_0	2.83	2.83	2.50	1.75	2.36	1.73	1.42	1.49	1.44	1.18

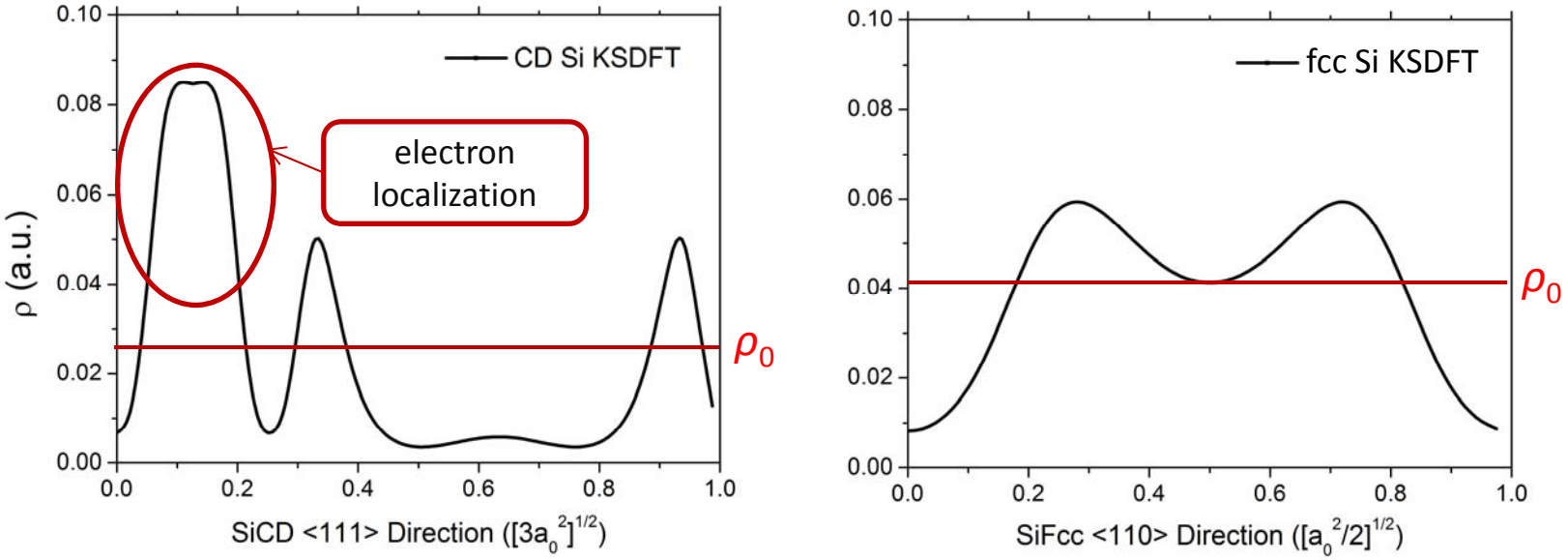

- WGC99 KEDF handles level of density fluctuation in hcp/bcc/fcc Si well.
- Large density fluctuations deviate from uniform electron gas limit, leading to WGC inaccuracies and a numerically unstable Taylor expansion.
- Idea: treat delocalized densities with WGC99; localized with semilocal KEDF

J. Xia and EAC, Phys. Rev. B **86**, 235109 (2012)

Decomposition of the density

$$\rho_{tot}(r) = \rho_{del}(r) + \rho_{loc}(r) \quad \rho_{del} = \rho_{total} \times F(\rho_{total} / \rho_0^{del}) \quad \rho_{loc}(r) = \rho_{tot}(r) - \rho_{del}(r)$$

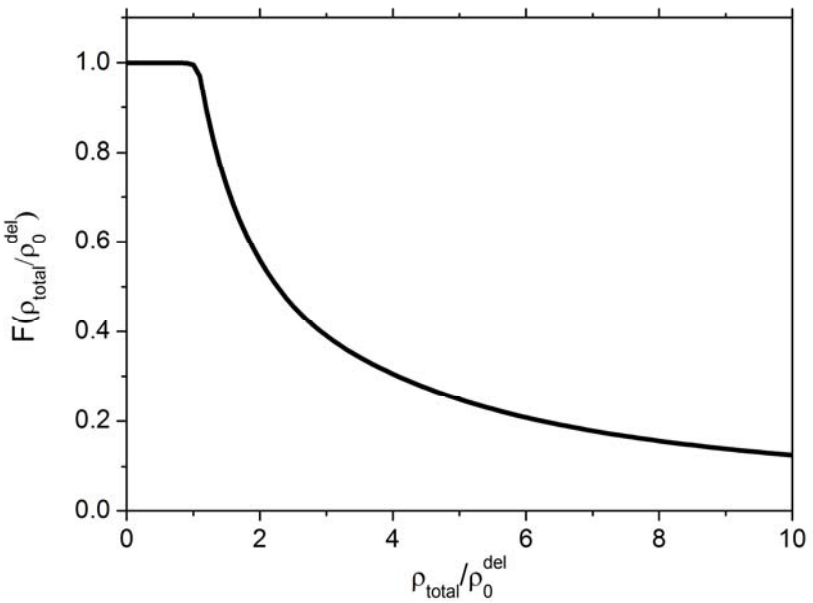

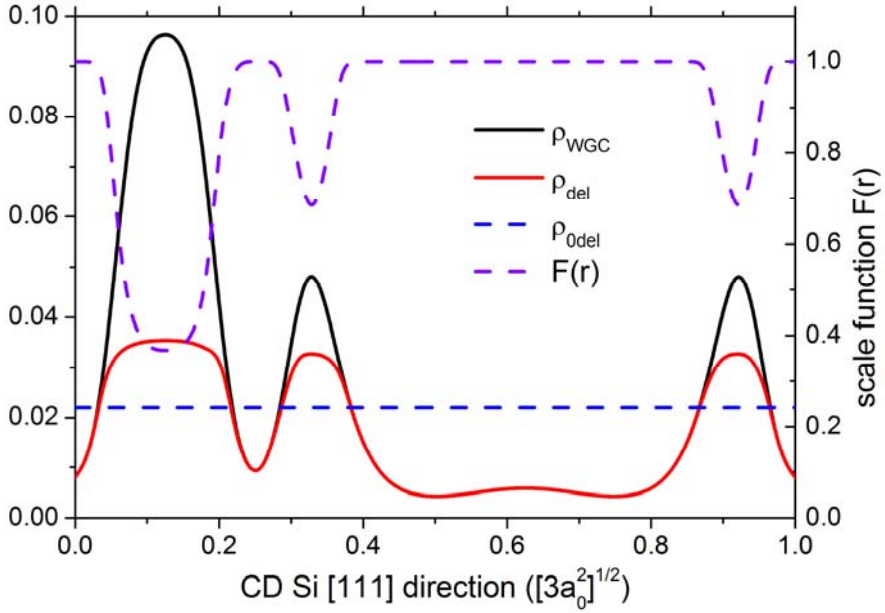

- Properties:
  - small $\rho_{total} \rightarrow$ large F; large $\rho_{total} \rightarrow$ small F.
  - Flat ρ_{del}, with $\rho_{max}^{del}/\rho_0^{del}$ <1.5
  - Two limits:

nearly-free-electron-like $\rightarrow \rho_{total} \approx \rho_0^{del} \rightarrow F(r) \approx 1 \rightarrow \rho_{del} \approx \rho_{total} \rightarrow WGC$

fully localized $\rightarrow \rho_{del}(r) \approx \rho_0^{del} \approx 0 \rightarrow \rho_{total}/\rho_0^{del} \approx \infty \rightarrow F(r) \approx 0 \rightarrow \rho_{del}(r) \approx 0 \rightarrow semilocal$

WGCD KEDF extends range of materials…

$$T_s[\rho_{total}] = T_s^{1}[\rho_{loc}] + (T_s^{1}[\rho_{total}] - T_s^{1}[\rho_{del}] - T_s^{1}[\rho_{loc}]) + T_s^{2}[\rho_{del}]$$

good for ρ_{loc} $\quad T_s^{1} = aT_{TF} + bT_{vW}$ $\qquad T_s^{2} = T_{TF} + T_{vW} + T_{WGC}$ good for ρ_{del}

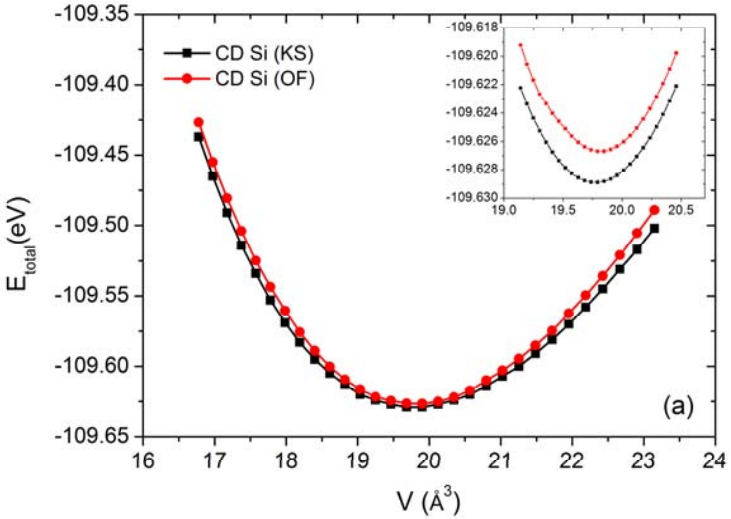

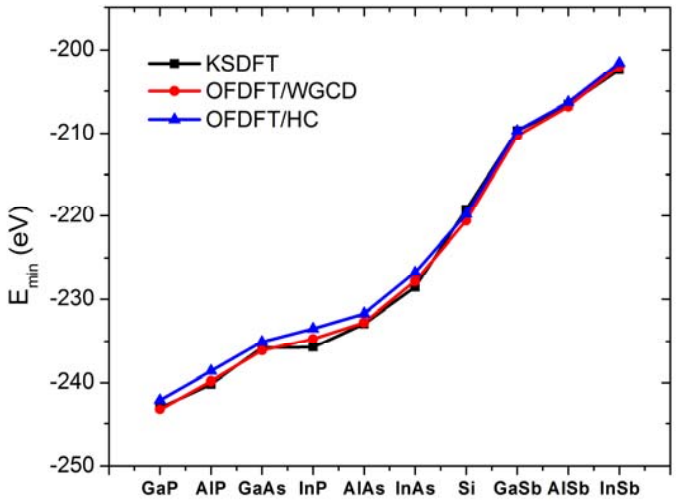

J. Xia and EAC, Phys. Rev. B **86**, 235109 (2012)

Plastic deformation of [111] Al nanowires

- After elastic limit, surface stresses nucleate plastic behavior at multiple locations along nanowire

- Initial yield mechanism highly dependent on nanowire diameter
  - 1 nm (1110 atoms): amorphous yielding
  - 2 nm (4170 atoms): amorphous yielding and shuffling
  - 4 nm (16770 atoms): yield along {111} slip planes

- Currently synthesized nanowires > 5 nm in diameter – predict yield along slip planes. Thinner wires cannot support dislocation motion => amorphization instead.

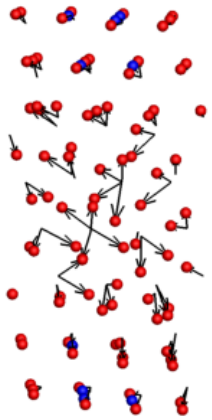

1 nm: Amorphous yielding (also observed in 2 nm nanowire)

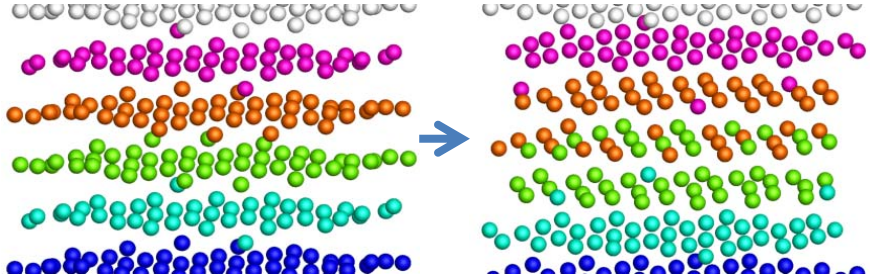

2 nm: 4 layers shuffle to form 5 layers to relieve strain. Colors identify the original layer.

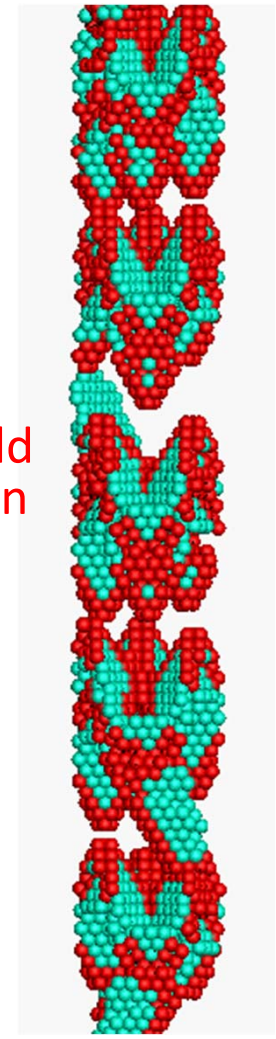

4 nm: slip planes form (figure shows only non-fcc, non-surface atoms)

L. Hung and EAC, J. Phys. Chem. C, **115**, 6269 (2011)

Summary

- Orbital-Free DFT as accurate as wavefunction-based Kohn-Sham DFT for main group metals, with nonlocal KEDFs and local pseudopotentials derived from Kohn-Sham DFT bulk crystal densities. (EAC papers 1999-2008)
- Nonlocal KEDFs built with correct physics of semiconductors extend range of materials accurately described by just density information (C. Huang & EAC, Phys. Rev. B **81**, 045206 (2010) and J. Xia & EAC, Phys. Rev. B **86**, 235109 (2012))
- Fully linear scaling and parallel OFDFT via FFTs, cardinal b-spline interpolation of the structure factor, domain decomposition => >1M atoms simulated with QM (L. Hung & EAC, Chem. Phys. Lett., **475**, 163 (2009).
- Angular momentum dependent OFDFT opens up the rest of the periodic table (transition metals, etc.) (Y. Ke, et al., Phys. Rev. Lett. **111**, 066402 (2013))
- Current applications: plasticity in metal alloys, Si-based Li ion batteries, liquid Li walls for fusion reactors, all via quantum mechanics without wavefunctions.

Acknowledgements

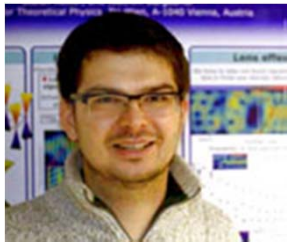

Prof. Florian Libisch (-> TU Wien)

Dr. Chen Huang (-> LANL)

Jin Cheng

Junchao Xia

Dr. Ilgyou Shin (-> Samsung)

Dr. Linda Hung (->U. of Illinois)

Max Kade Foundation, Inc.

NSF

DEPARTMENT OF THE NAVY
USN
ONR
Science & Technology

ARSC

TIGRESS
Terascale Infrastructure for Groundbreaking Research in Engineering and Science